International Journal of Mechanical Engineering and Robotics Research

ISSN 2278 – 0149 www.ijmerr.com
Vol. 3, No. 2, April 2014

Research Paper

SOLIDIFICATION OF IMPINGING MOLTEN METAL DROPLET ON A COLD SUBSTRATE

Amitesh Kumar[1]*

*Corresponding Author: Amitesh Kumar, ✉ amitesh_nifft@yahoo.com

The phenomenon of impingement and solidification of a molten metal droplet on a substrate occurs in processes like thermal spray coating and spray casting. Molten metal droplet after impingement over a substrate becomes a splat after spreading and solidification. The phenomenon of spreading and solidification of a droplet can be understood by mathematical modeling. In the present work, the spreading and solidification phenomenon of an impinging liquid metal droplet over a cold substrate are studied numerically using computational fluid dynamics software Fluent and validated experimentally. A model for heat transfer and solidification during impingement of a falling liquid Al-33wt%Cu droplet on a 304 stainless steel substrate has been developed. Al-33wt%Cu was selected so that Jackson-Hunt theory can be utilized for the validation of the impingement model.

Keywords: Metal droplet impingement, Solidification, Microstructure, Simulation

INTRODUCTION

The process of impingement of molten metal is complex and involves heat transfer, fluid flow and solidification. Droplet spreading is a free surface problem with large domain deformation in the presence of surface tension. The associated transient heat transfer processes involve convection with large temperature gradient in a deforming domain, liquid spread constrained by the multi-dimensional advancement of solidification interface, as well as the extraction of heat from a diminishing liquid region that is coupled with conduction in the substrate. The coupling between solidification and fluid dynamics can lead to non instinctive shapes (Waldvogel and Poulikakos, 1997). Experimental investigations of droplet solidification are quite challenging too, due to rapid change in shape and temperature as well as the small size of the droplet.

Most researchers in the 1960s and early 1970s focused on metallurgical aspects of the process, as evidenced in the review by Anantharaman and Suryanarayana (1971), Jones (1973), Jones (1982) and many of the

[1] Assistant Professor, National Institute of Foundry and Forge Technology, Hatia, Ranchi, India 834003.

existing heat transfer investigations of droplet impact ignore the fluid dynamics aspect of the process altogether.

Nichols *et al.* (1980) developed an alternative algorithm for solving complete Navier-Stokes equation in transient flow with multiple free surface. The method is called "Volume Of Fluid (VOF) method". Trapaga and Szekely (1991) used FLOW 3D, a commercially available code which implements the VOF methods to model three dimensional unsteady free surface flows, to study the isothermal impingement of liquid droplet in spraying process. Liu *et al.* (1993) studied the impingement of tungsten droplet by solving axisymmetric Navier-Stokes equations and the VOF equation. They used a RIPPLE code (Kothe et al., 1991).

Bennett and Poulikakos (1994) and Kang *et al.* (1994) studied droplet deposition assuming that solidification starts only after droplet spreading is complete and the splat is in the form of a disc. Theoretical and experimental studies done by Bennett and Poulikakos (1994) showed that the thermal conductivity of the substrate significantly affects the cooling rate of the splat. They did not incorporate the convection.

Using numerical models and experiments, Zhao *et al.* (1996a and 1996b) studied heat transfer and fluid dynamics during collision of a liquid droplet on a substrate. They extended the earlier model of Fukai *et al.* (1993) to account for the relevant convection and conduction heat transfer phenomena, both in the droplet and in the substrate, in the case, when there is no solidification. Their results, therefore, are applicable to the pre-solidification stage of the impact process. Liu *et al.* (1993) used a one-dimensional solidification model in conjunction with a two-phase flow continuum technique to track the moving liquid-solid boundary. The model, however, does not account for the convection in the liquid and conduction in the substrate.

Trapaga *et al.* (1992) used a commercially available code, FLOW-3DTM (Sicilian *et al.*, 1988), to study the heat transfer and solidification phenomena during droplet-impact. They assumed that the substrate was isothermal, and neglected any thermal contact resistance at the liquid-solid interface. Bertagnolli *et al.* (1997) used a finite element approach with an adaptive discretization technique to model the deformation of the droplet as well as the evolution of thermal field within the splat. Their model, however, does not take into account the solidification and heat transfer to the substrate. Liu *et al.* (1995) measured the temperature variation on the upper surface of an impacting metal droplet using a pyrometer, and used these results to estimate the thermal contact resistance under the drop. Wang and Matthys (1996) investigated the contact resistance effects experimentally and numerically for the droplet deposition. They described some new experimental results for copper splat cooling and estimated the interfacial thermal conductance between the molten copper and various cold substrates, and also the difference in conductance between liquid/solid contact and solid/solid contact. Chung and Rangel (2000) investigated numerically the contact resistance between the substrate and the splat and the undercooling effect at the two-dimensional phase change interface. Kamnis and Gu (2005) studied the case of droplet

impingement, when a powder particle is projected on substrate from a thermal spray gun to provide protective coatings. In this study they proved that the thermal contact resistance is the key parameter in characterizing the substrate surface roughness for impingement modeling and finally concluded that spreading, solidification and air entrapment are closely related to surface roughness. They validated their model using the experimental data of contact resistance between tin droplets and steel substrate. Shakeri and Chandra (2002) studied the splashing of molten tin droplet on a rough steel surface.

In the present work the development of a comprehensive mathematical model (that takes into account of impingement and solidification of molten droplet over a substrate) for the impingement of liquid Al-33Cu alloy droplet on a grade 304 stainless steel substrate has been attempted on FLUENT 6.3.16 platform. The present study also aims to validate the comprehensive model using Jackson and Hunt theory (1966) which relates the interlamellar spacing in solidified eutectic alloy with the solidification front velocity.

MODELING

Present study aims at developing a mathematical model of flow and heat transfer in a liquid metal which falls freely through gaseous medium and impinges on a cold substrate. Modeling of the phenomena is complex because it involves interactions among three phases, viz., liquid metal, solid substrate and gaseous medium. Further, as the droplet falls under the action of gravity and impinges on the substrate, its shape changes rapidly with time and its cooling is accompanied by solidification.

Figure 1 is a schematic sketch of the impingement phenomenon. With a symmetric boundary in the middle only half of the domain (ABFCDEA) was actually computed and a very fine grid was used for the regions where impact, spreading and solidification occur.

A droplet of Al-33wt%Cu, which is initially spherical, falls through the gaseous medium and impinges on a grade 304 stainless steel substrate. At the droplet/substrate interface a gap was created. This gap was used to model the interfacial contact resistance by prescribing an effective thermal conductivity to the gap. The thickness of the substrate was assumed to be 1 mm. Since the initial shape of the droplet is assumed to be spherical, the fluid flow and the heat transfer are axisymmetric (r-z direction).

The following assumptions have been made in the mathematical model:

- Spherical geometry Droplet is assumed up to just before the impingement.
- The problem is axi-symmetric about the axis shown in Figure 1.
- Impinge velocity of the droplet is perpendicular to the plane of the substrate.
- No rotation of droplet occurs along the axis.
- The flow of metal (droplet) and gas is laminar and incompressible. The velocity of gaseous media at domain walls is zero.
- Walls of the domain (Figure 1) are assumed to be at ambient temperature.
- The radiation from the droplet surface to the surroundings is ignored.

Figure 1: Schematic Representation of the Mathematical Model of Droplet Impingement

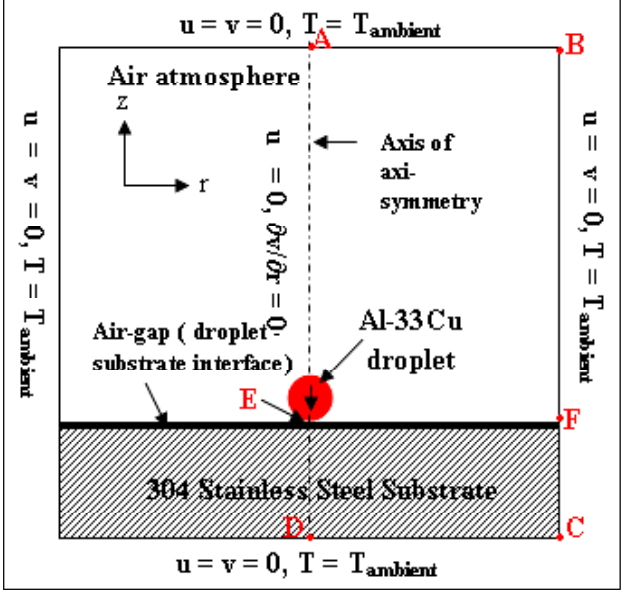

- To take into account the thermal contact resistance due to air gap a solid layer has been defined. The conductivity of the solid layer is estimated experimentally.
- Initial velocity of droplet (when it forms) is zero. It acquires velocity during the free fall. The velocity just before the impingement was $\sqrt{2gH}$, where H is the distance between the orifice of crucible and substrate.

Numerical simulations of the axis-symmetric droplet impingement processes were conducted by solving the 2-dimensional (r-z) continuity, Navier-Stokes and energy equations. The Volume Of Fluid (VOF) approach (Waldvogel and Poulikakos, 1997) was coupled with Navier-Stokes and energy equations to track the surface of the impinging droplet on a fixed eulerian structured mesh.

Solidification results in latent heat generation and a modified form of the energy equation, incorporating latent heat have been used. The modified energy equation is given by

$$\frac{\partial}{\partial t}(\rho H)+\nabla\cdot(\rho u H)=\nabla\cdot(k\,\nabla T)+S_h \qquad ...(1)$$

where H is the enthalpy per unit volume, k is thermal conductivity and S_h is the rate of energy generation per unit volume. The enthalpy of the material was computed as the sum of the sensible enthalpy, h, and the latent heat, ΔH. It is expressed as

$$H = h + \Delta H \qquad ...(2)$$

where,

$$h = h_{ref} + \int_{T_{ref}}^{T} c_P dT \qquad ...(3)$$

In Equation (3) h_{ref} is the sensible enthalpy at the reference temperature and C_P is the specific heat at constant pressure.

The liquid fraction, β, is defined as:

$$\beta = 0 \quad \text{if } T < T_{solidus}$$
$$\beta = 1 \quad \text{if } T > T_{liquidus}, \qquad ...(4)$$
$$\beta = \frac{T - T_{solidus}}{T_{liquidus} - T_{solidus}} \text{ if } T_{solidus} < T < T_{liquidus}.$$

The latent heat content can be written in terms of the latent heat of freezing, L:

$$\Delta H = \beta L \qquad ...(5)$$

The source term appearing on the right-hand side of Equation (1) is given by

$$S_h = \frac{\partial(\rho\Delta H)}{\partial t} + \nabla(\rho u \Delta H) \qquad ...(6)$$

Due to high temperature difference between the droplet and substrate and the relatively low droplet velocity, viscous dissipation of heat

was negligible and thus not included in the source term.

Solidification results in phase change. Instead of tracking the interface, Al-33 wt%Cu was assumed to be a single phase pseudo-porous medium whose porosity was taken as proportional to the liquid fraction. Thus the porosity of this single phase pseudo-porous medium varied from zero in the solidified region to one in the completely liquid region. However, Al-33wt%Cu is a eutectic alloy and thus a sudden transition in the porosity is expected at the solidification front. To avoid numerical difficulties associated with this sudden transition the solidification front was assumed to be a narrow band and the porosity was varied from zero one over this band. The effect of porosity was incorporated in the momentum equations through a momentum source terms.

All zones were initialized with the temperature of 300 K, except the droplets. The droplets were set to a predetermined higher temperature. The initial velocities at every point inside the domain were zero, except within the droplets.

Since problem is axis-symmetric only half of the domain shown in Figure 1 was considered in the computation domain. Axis of symmetry was like a free-slip wall. The normal velocity was zero. Tangential velocity did not have normal gradient. Thus along the axis of axis-symmetry $u = 0$ and $\partial v/\partial r = 0$. At the other boundaries $u = 0$ and $v = 0$. Since these boundaries are far away from the droplet, the temperatures at these boundaries were set equal to the ambient temperature, i.e., 300 K. The above described model was simulated using FLUENT 6.3.16 plat form.

Thermo-physical properties of Al-33wt%Cu that have been used for simulation are given in Table 1. Table 2 provides the thermo-physical properties of the grade 304 stainless steel.

Table 1: Thermo-Physical Properties of Al-33Cu Alloy

Properties of Al-33wt%Cu Used in Model	**Value**
Thermal conductivity ($Wm^{-1} K^{-1}$)	K_s = 155 K_l = 71
Density ($kg\ m^{-3}$)	ρ_s = 3410 ρ_l = 3240
Solidus Temperature (K)	821
Liquidus Temperature (K)	821
Melting Heat ($J\ Kg^{-1}$)	350000
Specific Heat ($J\ Kg\ K^{-1}$)	C_s =1070 C_l = 895
Viscosity* ($kg\ m^{-1}\ s^{-1}$)	at 943 K = 1.001×10^{-3} (Korol'kov, 1960) at 973 K = 8.624×10^{-4} (Korol'kov, 1960) at 1023 K = 5.65×10^{-4} (Korol'kov, 1960)
Surface Tension ($N\ m^{-1}$)	0.868 (Lang, 1974)

Note: s = solid; l = liquid;

*Value of viscosity of Al33wt%Cu has been calculated using Arrhenius equation: $\mu = \mu_0 \exp(\frac{E}{RT})$ up to the solidus temperature.

Table 2: Thermo-Physical Properties of 304 Stainless Steel Alloy

Properties of Grade 304 Stainless Steel	**Value**
Thermal Conductivity ($Wm^{-1} K^{-1}$)	15
Density ($kg\ m^{-3}$)	7900
Specific Heat ($J\ Kg^{-1}\ K^{-1}$)	477

Contact resistance was estimated using the inverse modeling approach and its value was estimated to be 7×10^{-4} m^3-K/w. The details of

this are given in the paper by Kumar *et al.* (2010).

EXPERIMENTS FOR VALIDATION OF MODEL

A droplet impingement set up to validate the model was fabricated. Figure 2 shows the schematic sketch of the set-up.

A vertical resistance furnace was used for melting. The furnace has a cylindrical shape having a height of 8 inch, an outer diameter of 4 inch and an inner diameter of 1 inch. The temperature of the melt could be controlled within ±5 °C. It was placed at the top of the droplet impingement chamber as shown in Figure 2. A quartz tube with an inner diameter of 17 mm was used as a crucible. At the bottom of the crucible there was a melt delivery nozzle. The diameter of the melt delivery nozzle was 2 mm. Substrate was made of grade 304 stainless steel. The substrate was circular in shape having a diameter of 20 cm and thickness of 20 mm. It was placed inside the spray chamber. Pieces of master alloy Al-33Cu were melted in the quartz crucible. The temperature of the melt was maintained at ~150 °C above the melting point. By application of air pressure droplets were pushed out of the 2 mm diameter melt delivery nozzle. These droplets impacted on the substrate, deformed and finally solidified on it. For deposited splats, the size of the droplet was estimated by measuring the weight of splats. The microstructural characterizations of the deposited droplets were carried out using standard metallographic procedures.

Figure 2: Schematic Sketch of Droplet Impingement Set Up

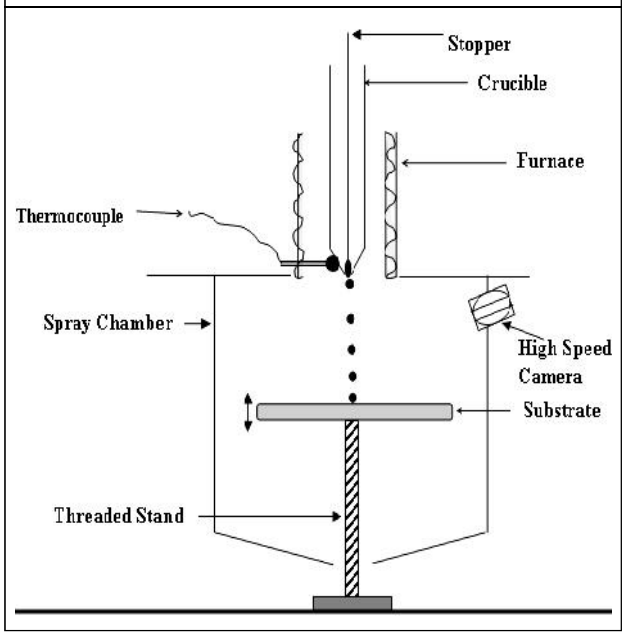

JEOL JSM-5800 Scanning Microscope and Field Emission Scanning Electron Microscope (Model: Carl Zeiss SMT Ltd.) were used for taking the microstructure at higher magnifications. The interlamellar spacing (^{a}) of the eutectic structure of Al-33Cu was measured by drawing perpendicular line using Optical Image Analyzer Leica DMLM.

RESULTS AND DISCUSSION

Simulation of Droplet Impingement

In the present study simulations were carried out for the droplets of diameter 5.39 mm falling through a height of 50 cm on a grade 304 stainless steel substrate. The substrate thickness was taken as low as 1mm in order to reduce the computational time. This will not affect the accuracy of the prediction of the thermal field because during the short duration of droplet spreading and solidification the temperature rise in the substrate did not take place beyond a distance of 0.2 mm.

The computed velocity, temperature, liquid fraction and phase (Al-33Cu and air) fields were plotted at different time intervals by

simulation of the impingement model on FLUENT 6.3.16 platform. Figure 3 shows the phase contour of Al-33Cu droplet having a diameter of 5.39 mm in air. In this case the velocity of impingement was 3.13 ms^{-1}. Therefore the Weber number was 207. The spread of the droplet occurred within a short time frame of 5.0 ms and no disintegration due to the surface tension force was observed. It can also be seen that the solidification starts 10.0 ms after the spread has taken place. Figure 4 also shows the velocity profile of Al-33Cu/air system. It can be noted from the figure that air adjacent to Al-33Cu, is dragged in the direction of spread and a re-circulating flow in the air can be observed.

Droplet spreads radially after impingement on the substrate along the surface of the substrate as shown in the phase profile (Figure 3) and velocity profile (Figure 4). Thin solidification layers were developed at the edge of the droplet 10 ms after the impact; the solidification layers progressed to the most of the contact surface as the droplet spreaded at 20 ms; and full solidification finished at 76 ms. The phase contour and velocity vector results are shown in Figures 3 and 4, respectively. On impact, the high impact velocity generates a high pressure region under the droplet; forced the liquid to flow over the contact surface while the effect of surface tension was comparatively less; the maximum flow velocity was achieved at the edge where all the momentum was transferred to the radial direction and the cross-section area was small. The velocity at the edge was found to be 5.59 ms^{-1} after 1.0 ms which is higher than the impact velocity of 3.13 ms^{-1}. With the spreading and solidification progressed, the flow of liquid metal reduced and the effect of surface tension became significant, which generated high pressure regions at the edges and finally reversed the flow back towards the centre as shown in the 8.0 ms time frame plot

Figure 3: Phase Profile of Impinging Al-33Cu Droplet on the Substrate

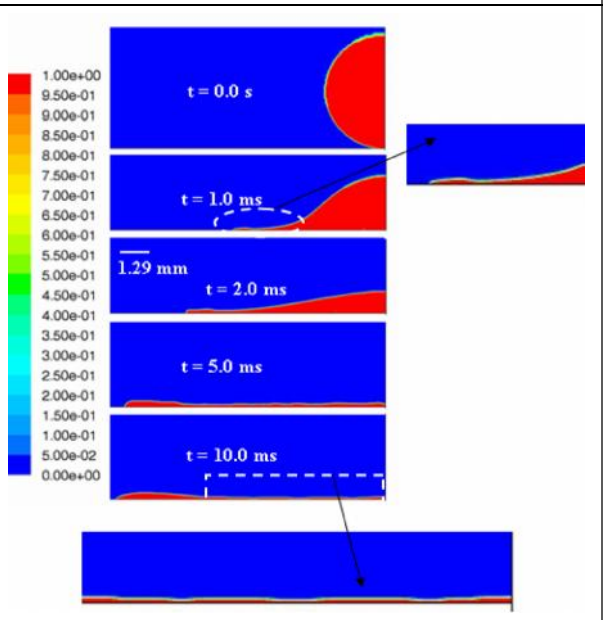

Figure 4: Velocity Profile of the Al-33Cu / Air System

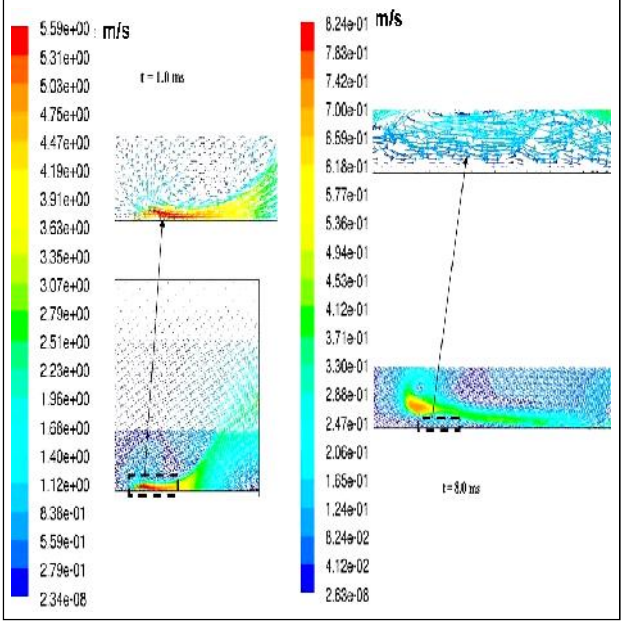

in Figure 4. This resulted into the formation of bump at the edge of the splat.

The simulated evolution of droplet shape (Figure 3) has been reported earlier (Fukai *et al.*, 2000). The bump near the edge has been observed even when there is no cooling (Sikalo and Ganic, 2006). The physical reasons for the bump formation are not fully understood although surface tension and the existence of the bump because of the maximum cooling near the edge (Figure 5) (Fukai *et al.*, 2000) could be suggested as two of the reasons.

The thermal contour in Figure 5 shows convective cooling at the top surface, where Al-33Cu is cooler than the inner region.

Figure 5: Temperature Profile of Impinging Al-33Cu Droplet on the Substrate

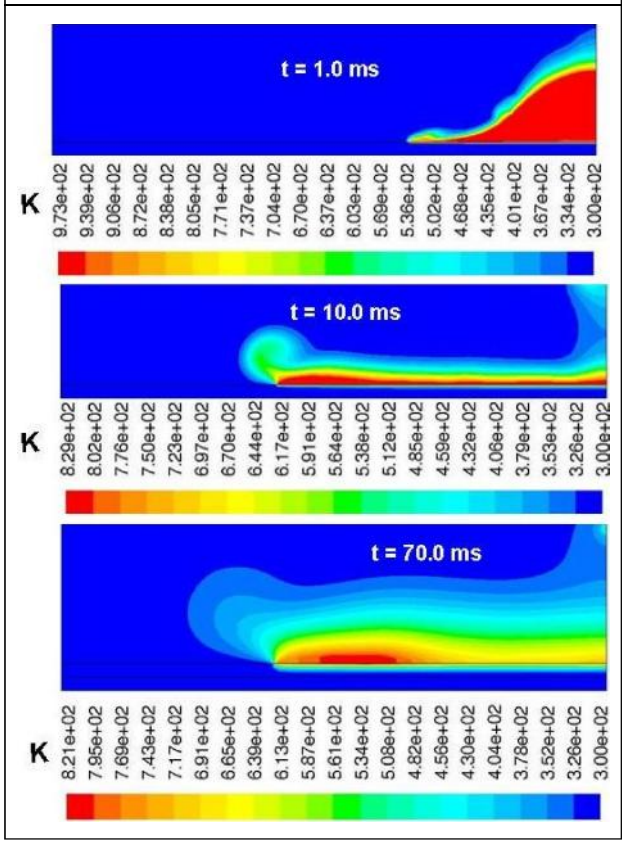

Similarly conductive cooling of Al-33Cu near the substrate can be seen along with heating up of the substrate as shown in the temperature profile plotted (Figure 5). Figure 6 shows the liquid fraction within Al-33Cu system.

Figure 6: Liquid Fraction Profile of Al-33Cu / Air System

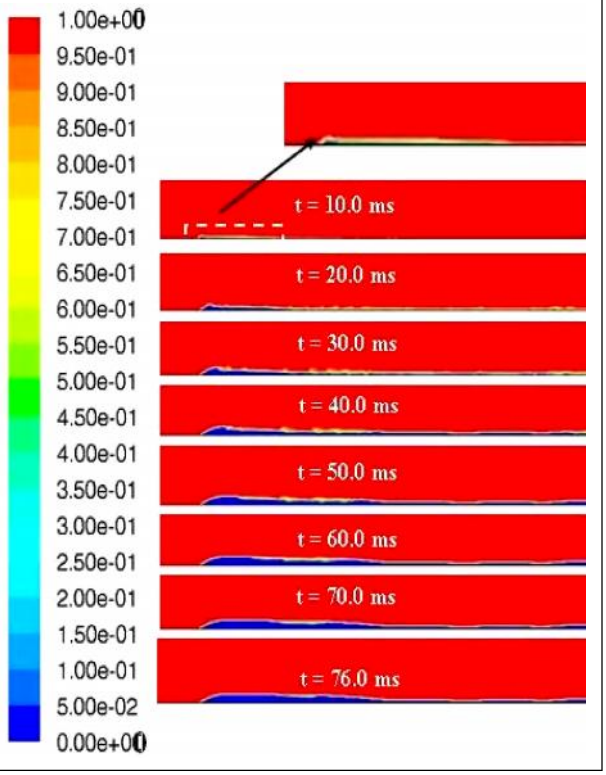

Estimation of Solidification Front Speed

From the liquid fraction profile the position of the solidification front can be tracked. It can be observed that the front is almost parallel to the substrate and therefore the heat transfer must be predominated by the substrate cooling.

When a solidification layer grows, the lower part of the liquid splat loses momentum as it solidifies to become a part of solidified layer. Solidification may take place during spreading,

but the solidified layer growth velocity is slow compared to when solidification starts after complete spread. Therefore, a splat retains radial momentum during spreading and reaches its maximum diameter while solidifying.

Solidification front speed was estimated based on the liquid fraction profile at 10 different locations. Figure 7 shows the different locations in the splat along the radial direction. The simulated front speed of solidification of the splat was determined from variation of liquid fraction profile with time. The ratio of solidified thickness to elapsed time gives the front speed of the splat solidification. The splat solidification is almost unidirectional, it starts from the interface of the substrate and the effect of convection is negligible as compared to the conduction. The front speed was not found to be fixed across the cross section. It is mainly due to variation in thickness of splat (Kumar *et al.*, 2010).

VALIDATION OF THE MODEL

The experimental validation was carried out for a droplet of diameters 5.39 mm and having a superheat of 150 K (initial temperature = 973 K). The solidified droplets were sectioned at different locations (Figure 7) and the sectioned pieces were metallographically prepared to characterize the microstructure. Microstructures of 5.39 mm droplet deposited over substrate are shown in the Figure 8.

For validation, solidification front velocities in droplet having diameter of 5.39 mm were calculated using the model developed in the present work. These values were plugged in the Jackson-Hunt relationship ($^{a^2}V = 88\ \mu m^3/s$) (Jones, 1982) for calculation of ë from those velocities. Figure 9 shows the experimental values obtained for various sections which are shown in Figures 7 and 8 superimposed on

Figure 7: Profile of Deformed Droplet Location for Determination of Cooling Rate at Different Positions

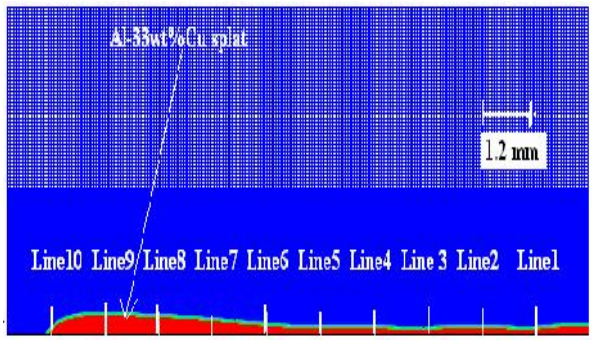

Figure 8: Lamellar Eutectic Microstructure of 5.39 mm Diameter Droplet

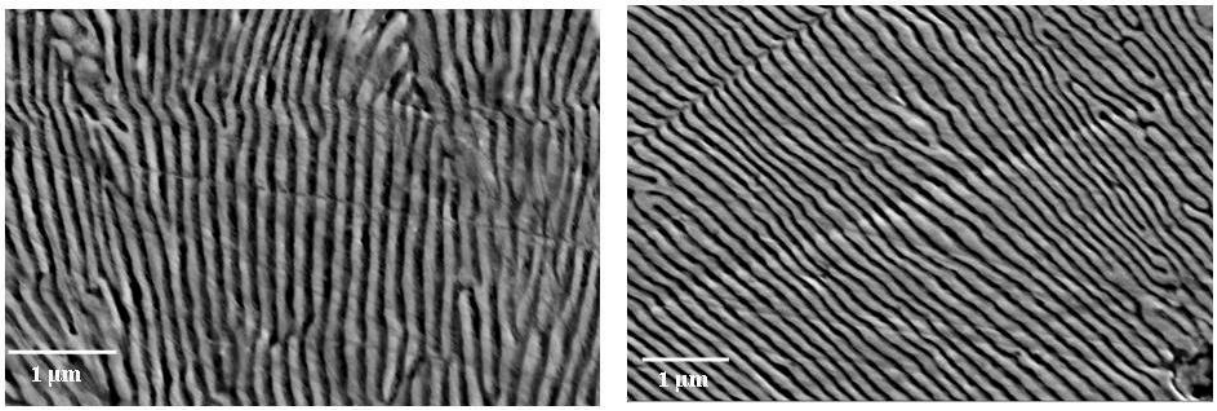

Figure 9: Interlamellar Spacing versus Growth Velocity

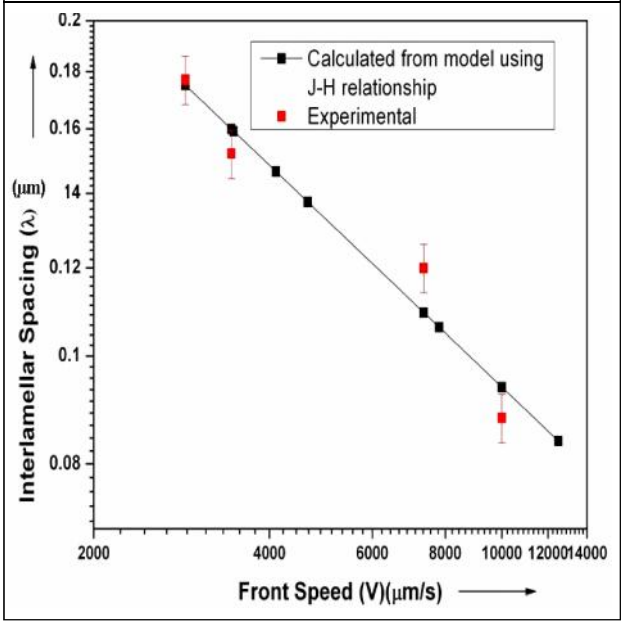

those the ones calculated from this model. A very good correlation can be seen in the plot between experimental and simulated values within standard errors of experimental measurements.

CONCLUSION

The droplet impingement and solidification model was simulated for droplet of diameter 5.39 mm, initial droplet temperatures of 973 K, and impingement velocities of 3.13 ms^{-1}. The simulation carried out for droplet (diameter = 5.39 mm, impinging velocity = 3.13 ms^{-1}, initial temperature = 973 K) suggests the following.

- The spread of the droplet occurred within a short time frame of 5.0 ms and no disintegration and observed that the solidification starts 10.0 ms after the spread has taken place.
- On impact, the maximum flow velocity was achieved at the edge where all the momentum was transferred to the radial direction and the cross-section area was small. The velocity at the edge was found to be 5.59 ms^{-1} after 1.0 ms which is higher than the impact velocity which was 3.13 ms^{-1}. As the spreading and solidification progressed, the flow of liquid metal reduced and the effect of surface tension became significant, which generated high pressure regions at the edges and finally reversed the flow back towards the centre. This resulted into the formation of bump at the edge of the splat.
- The prediction of the model on droplet spreading matched well with the experimental findings and so did the prediction of the interlamellar spacings at different locations of the splat.

REFERENCES

1. Anantharaman T R and Suryanarayana C (1971), "Review: A Decade of Quenching from the Melt", *Journal of Material Science*, Vol. 6, pp. 1111-1135.
2. Bennett T and Poulikakos D (1994), "Heat Transfer Aspects of Splat-Quench Solidification: Modeling and Experiments", *Journal of Material Science*, Vol. 29, pp. 2025-2039.
3. Bertagnolli M, Marchese M, Jacucci G, St. Doltsinis I and Noelting S (1997), "Thermo-Mechanical Simulation of the Splashing of Ceramic Droplets on a Rigid Substrate", *Journal of Computational Physics*, Vol. 133, No. 2, pp. 205-221.
4. Chung M and Rangel R H (2000), "Simulation of Metal Droplet Deposition with Solidification Including Undercooling and Contact Resistance Effects",

Numerical Heat Transfer, *Part A*, Vol. 37, No. 3, pp. 201-226.

5. Chung M and Rangel R H (2000), "Simulation of Metal Droplet Deposition with Solidification Including Undercooling and Contact Resistance Effects", *Numerical Heat Transfer, Part A*, Vol. 37, No. 3, pp. 201-226.
6. Fukai J, Ozaki T, Asami H and Miyatake O (2000), "Numerical Simulation of Liquid Droplet Solidification on Substrate", *Journal of Chemical Engineering of Japan*, Vol. 33, No. 4, pp. 630-637.
7. Fukai J, Zhao Z, Poulikakos D, Megaridis C M and Miyatake O (1993), "Modeling of the Deformation of a Liquid Droplet Impinging Upon a Flat Surface", *Physics of Fluids A*, Vol. 5, pp. 2588-2599.
8. Fukumoto M, Nishioka E and Matsubara T (1999), "Flattening and Solidification Behavior of a Metal Droplet on a Flat Substrate Surface Held at Various Temperatures", *Surface and Coatings Technology*, Vols. 120-121, pp. 131-137.
9. Jackson K A and Hunt J D (1966), "Lamellar and Rod Eutectic Growth", *Transactions of the Metallurgical Society of AIME*, Vol. 236, pp. 1129-1142.
10. Jones H (1973), "Splat Cooling and Metastable Phases", Report of Progress in Physics, Vol. 48, pp. 1425-1497.
11. Jones H (1982), "Rapid Solidification of Metals and Alloys", No. 8, The Institution of Metallurgists, London.
12. Kamnis S and Gu S (2005), "Numerical Modelling of Droplet Impingement", *Journal of Physics D: Applied Physics*, Vol. 38, pp. 3664-3673.
13. Kang B, Zhao Z and Poulikakos D (1994), "Solidification of Liquid Metal Droplets Impacting Sequentially on a Solid Surface", *Journal of Heat Transfer*, Vol. 116, pp. 436-445.
14. Korol'kov A M (1960), "Casting Properties of Metals and Alloys", pp. 64-66, Consultants Bureau, New York.
15. Kothe D B, Mjolsness R C and Torrey M D (1991), "RIPPLE: A Cornputer Program for Incompressible Flows with Free Surfaces", Los Alamos Scientific Laboratory, LA-12007- MS, UC-000.
16. Kumar A, Ghosh S and Dhindaw B K (2010), "Simulation of Cooling of Liquid Al-33wt%Cu Droplet Impinging on a Metallic Substrate and its Experimental Validation", *Acta Materialia*, Vol. 58, pp. 122-133.
17. Lang G (1974), "Effect of Addition Elements on the Surface Tension of Liquid Very High Purity Aluminum", *Aluminium*, Vol. 50, No. 11, pp. 731-734.
18. Liu H, Lavernia E J and Rangel R H (1993), "Numerical Simulation of Substrate Impact and Freezing of Droplets in Plasma Spray Processes", *Journal of Physics D: Applied Physics*, Vol. 26, pp. 1900-1908.
19. Liu H, Lavernia E J and Rangel R H (1995), "Modeling of Droplet-Gas Interaction in Spray Atomization of Ta-2.5 W Alloy", *Materials Science and Engineering A*, Vol. 191, pp. 171-184.

20. Nichols B D, Hirt C W and Hotchkiss R S (1980), "SOLA-VOF: A Solution Algorithm for Transient Fluid Flow with Multiple Free Boundaries", Los Alamos Scientific Laboratory, LA-8355, UC-32 and UC-34.

21. Shakeri S and Chandra S (2002), "Splashing of Molten Tin Droplets on a Rough Steel Surface", *International Journal of Heat and Mass Transfer*, Vol. 45, pp. 4561-4575.

22. Sicilian J M, Hirt C W and Harper R P (1988), "FLOW-3D: Computational Modeling Power for Scientists and Engineers" (FLOW-3D, Report No. FSI-88-00-1, Flow Science Inc., Los Alamos, NM, Vols. 1-4, 1988).

23. Sikalo S and Ganic E N (2006), "Phenomena of Droplet-Surface Interaction", *Experimental Thermal and Fluid Science*, Vol. 31, pp. 97-110.

24. Trapaga G and Szekely J (1991), "Mathematical Modeling of the Isothermal Impingement of Liquid Droplets in Spraying Processes", *Metallurgical Transactions B*, Vol. 22, pp. 901-914.

25. Trapaga G, Matthys E F, Valencia J J and Szekely J (1992), "Fluid Flow, Heat Transfer and Solidification of Molten Metal Droplets Impinging on Substrates: Comparison of Numerical and Experimental Results", *Metallurgical Transactions B*, Vol. 23, pp. 701-718.

26. Waldvogel J M and Poulikakos D (1997), "Solidification Phenomena in Picoliter Size Solder Droplet Deposition on a Composite Substrate", *International Journal of Heat and Mass Transfer*, Vol. 40, No. 2, pp. 295-309.

27. Waldvogel J M and Poulikakos D (1997), "Solidification Phenomena in Picoliter Size Solder Droplet Deposition on a Composite Substrate", *International Journal of Heat and Mass Transfer*, Vol. 40, No. 2, pp. 295-309.

28. Wang G X and Matthys E F (1996), "Experimental Investigation of Interfacial Thermal Conductance for Molten Metal Solidification on a Substrate", *Journal of Heat Transfer*, Vol. 118, pp. 157-163.

29. Yang Y-S, Kim H Y and Chun J H (2003), "Spreading and Solidification of a Molten Microdrop in the Solder Jet Bumping Process", *IEEE Transactions on Components and Packaging Technologies*, Vol. 26, No. 1, pp. 215-221.

30. Zhang H (1999), "Theoretical Analysis of Spreading and Solidification of Molten Droplet During Thermal Spray Deposition", *International Journal of Heat and Mass Transfer*, Vol. 42, pp. 2499-2508.

31. Zhao Z, Poulikakos D and Fukai J (1996a), "Heat Transfer and Fluid Dynamics During the Collision of a Liquid Droplet on a Substrate-I, Modeling", *International Journal of Heat and Mass Transfer*, Vol. 39, pp. 2771-2789.

32. Zhao Z, Poulikakos D and Fukai J (1996b), "Heat Transfer and Fluid Dynamics During the Collision of a Liquid Droplet on a Substrate-II, Experiments", *International Journal of Heat and Mass Transfer*, Vol. 39, pp. 2791-2802.